Heliyon 8 (2022) e10853

Contents lists available at ScienceDirect

Heliyon

journal homepage: www.cell.com/heliyon

Research article

The role of electrochemical potentials of solid-state energy emissive harvesters

J.J. Fernández

Departamento de Física Fundamental, Universidad Nacional de Educación a Distancia (UNED), 28040 Madrid, Spain

HIGHLIGHTS

- All energy-emissive harvesters can be described using a common physical model.
- The particle conservation model if used in energy-emissive converters can lead to wrong results.
- The incorporation of Intermediate Bands in thermoradiative cells will not improve their performance.

ARTICLE INFO

Keywords:
Core radiative material
Cold-carrier energy-emissive harvester
Thermoradiative cell
Intermediate-band thermoradiative cell

ABSTRACT

We prove that semiconductor and metallic energy-emissive harvesters, thermoradiative cells and intermediate-band thermoradiative cells are obtained from the concept of core radiative material doing different approximations. We also show that using this concept it is possible to predict new outcomes on energy-emissive harvesters. Among the new results we highlight the possible failure of the particle conservation model if used on cold-carrier energy emissive harvesters, that intermediate band solar cells must produce small output powers and the reduction of the cell power of thermoradiative cells due to multiexcitonic processes. Moreover, we explain the physical principles of the differences found between results obtained using the detailed balance method and results that are obtained without using it.

1. Introduction

We use a general framework to study different kinds of energy-emissive harvesters (EEHs) such as cold-carrier energy-emissive harvesters (CC-EEHs), thermoradiative cells (TRCs) and intermediate-band thermoradiative cells (IB-TRCs). EEHs were proposed in 2014 by Byrnes et al. [1] and are devices able to produce electric output power using their own emission of radiation. Byrnes' work is the result of several years of studies on the physical properties of radiative cooling materials and structures [2, 3, 4, 5, 6, 7, 8, 9, 10, 11].

As EEHs are hotter than their surroundings, because they receive heat from an external source, they are able to transform a part of the received heat into electrical power and, at the same time, to radiate the other part of it to their surroundings. EEHs are implemented either using energy-selective contacts (CC-EEHs) or semiconductor p-n junctions (TRCs) [1, 12, 13, 14, 15, 16, 17, 18, 19, 20, 21, 22, 23, 24, 25, 26, 27, 28, 29, 30, 31, 32, 33, 34]. CC-EEHs are implemented using metallic emitters (metallic CC-EEHs) and semiconductor ones (semiconductor CC-EEHs).

CC-EEHs and TRCs are the most simple implementations of EEHs as they are the counterparts of hot carrier solar cells (HCSCs) and photovoltaic cells [12] [13]. As discussed in the literature, the implementation of TRCs and CC-EEHs face two important challenges [1], [35], [25]. For TRCs it is necessary to find out suitable materials with a small bandgap of less than 0.3-0.4 eV and a small rate of non-radiative recombinations. For CC-EEHs the challenge is the fabrication of the energy-selective contacts (ESCs) [12]. Moreover, for both types of EEHs it is necessary to find out materials that do no degrade when the cell works at high temperatures.

We think that the implementation of CC-EEHs is possible as the necessary requirement of having slow carrier cooling in the cell emitter is achieved using materials such as InP and InN [36] [37]. As reported in those two works the slowdown of the de-excitation processes is reached using materials with a big phononic bandgap that prevents the Klemens decay of optical phonons into acoustic modes [38]. Another form to slow-down the electronic de-excitations is to use materials where the decay of optical phonons into a sum of longitudinal and transverse acoustic phonon modes is avoided [39].

E-mail address: jjfernandez@fisfun.uned.es.

https://doi.org/10.1016/j.heliyon.2022.e10853
Received 22 March 2022; Received in revised form 16 June 2022; Accepted 26 September 2022

In this work we propose a general theoretical concept, the *core radiative material* (CRM) from which the concepts of semiconductor and metallic CC-EEH, TRC and IB-TRC are deduced doing different approximations. Our formalism is based on the one proposed by Luque et al. for photovoltaic cells [40]. So, we only discuss on the adaptation of the method to the case of EEHs. We highlight that the adaptation to EEHs is what differentiates our work from Luque's one. Then, using the concept of CRM we predict the general behaviour of some systems that have not been studied such as TRCs where multiexciton processes are important or terrestrial IB-TRCs working connected to very cold environments.

Our work organises as follows. In section 2 we present the concept of CRM that will serve as the vehicle to understand the working properties of different types of EEHs. Then, in section 3 we use the concept to explain properties of CC-EEHs and to check that our model reproduce the results of previous works on metallic and semiconductor CC-EEHs. In section 4 we use the formalism to discuss the effect of the impact ionization on TRCs. In section 5 we present a brief discussion about the real possibilities of making intermediate-band TRCS (IB-TRCs) and what we expect from their functioning. We end this work with a summary of our discussion.

Thus, the main targets of this work are,

- To present a common framework to study all types of EEHs.
- To show that in the new framework several of the results presented in the literature can be easily explained and that they have common physical grounds.
- To predict new results on EEHs.

2. General theoretical framework

Here we adapt the formalism used by A. Luque et al. [41] to study photovoltaic energy converters to establish a general framework that allows the study of metallic and semiconductor CC-EEHs, TRCs based on pn-juntions where the impact ionization is negligible, and others where this mechanism plays an important role. We also study IB-TRCs.

The CRM is formed by two sets of states like those shown in the panels (a)-(c) of Fig. 1. One of the sets has low energies ε_i below a forbidden region (bandgap) of energy width E_G and is associated to the valence band (VB) of semiconductors. The other set is formed by states of energy $\varepsilon_j > E_G$ and is associated to the conduction band (CB) of semiconductors. For semiconductor systems the two states are separated in energy by E_G. In metallic systems $E_G = 0$ so the two groups of states are not separated in energy.

The electronic interactions that happen in the CRM are written-down as,

$$e_1 + e_2 \leftrightarrows e_3 + e_4. \tag{1}$$

In equation (1) e_1, e_2, e_3 and e_4 represent different electrons. This equation is also written down in terms of the energies ε_1, ε_2, ε_3 and ε_4 of the electrons as,

$$\varepsilon_1 + \varepsilon_2 \leftrightarrows \varepsilon_3 + \varepsilon_4 + \Delta\varepsilon. \tag{2}$$

Here the term $\Delta\varepsilon$ is introduced to account for $e^- - e^-$ interactions that do not preserve the energy. In EEHs this term is very small and represents the energy that is dispersed to the lattice when $e^- - e^-$ interactions happen. Moreover, it is also interesting to write the $e^- - e^-$ interaction as an equilibrium condition of the chemical potentials,

$$\mu_1 + \mu_2 \leftrightarrows \mu_3 + \mu_4. \tag{3}$$

We note now that equations (2) and (3) can only be satisfied at the same time if the relation between the energies ε_i $(i = 1, ..., 4)$ and the chemical potentials μ_i $(i = 1, ..., 4)$ is linear,

$$\mu_i = a + b\varepsilon_i, \tag{4}$$

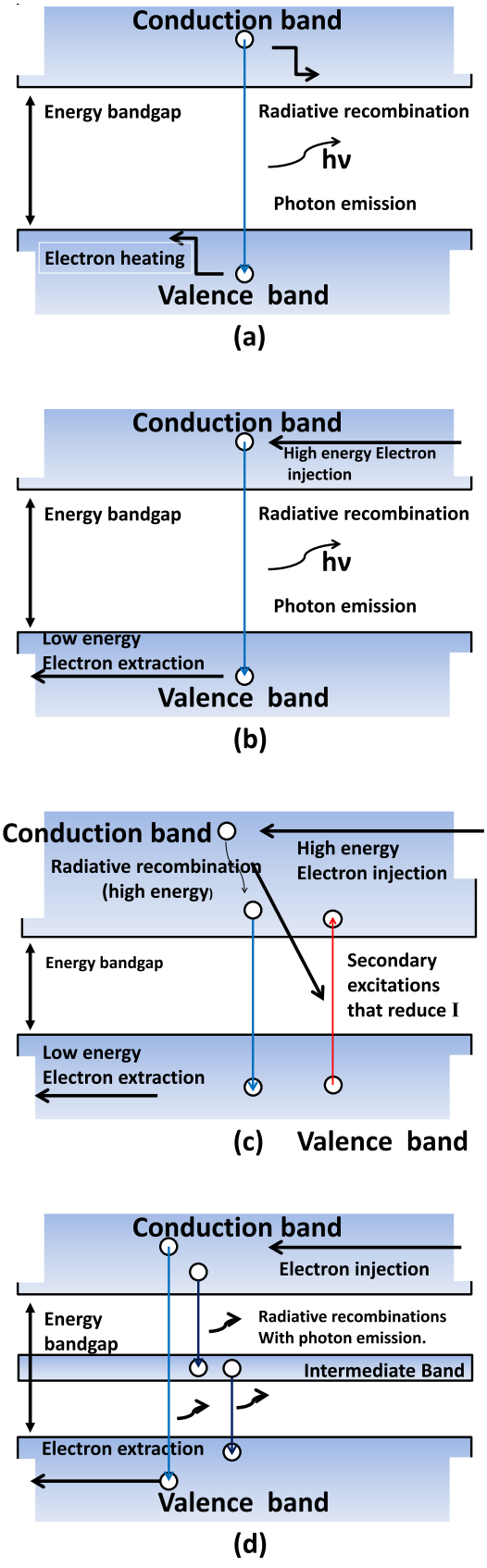

Fig. 1. Shematic diagram of the CRM showing the mechanisms involved in (a) single bandgap TRCs. (b) CC-EEHs. (c) TRCs with a small bandgap where secondary excitations happen. (d) Intermediate band thermoradiative cells. In each diagram we show the most relevant mechanisms involved in the operation.

where the coefficients a and b are constants.

Using (4) it is possible to rewrite the Fermi-Dirac electronic distribution in the material

$$f_{FD} = \frac{1}{\exp\left[\frac{\varepsilon - \mu_i}{KT}\right] - 1} = \frac{1}{\exp\left[\frac{\varepsilon - (a - b\varepsilon_i)}{KT}\right] - 1}. \quad (5)$$

Where in equation (5) K is the Boltzmann constant and T is the temperature, as

$$f_{FD} = \frac{1}{\exp\left[\frac{\varepsilon - \mu_e}{KT'}\right] - 1}. \quad (6)$$

In (6) we have defined (i) the electronic effective potential

$$\mu_e = \frac{b}{1-a} \quad (7)$$

and (ii) the effective temperature

$$T' = \frac{T}{1-a}, \quad (8)$$

Equations (7) and (8) were deduced by Würfel [42] [43] studying the electronic populations of HCSCs. They are general, and therefore valid in the context of EEHs. However, they are applied differently to EEHs and HCSCs. Thus, while in HCSCs the coefficients a and b are positive numbers, in EEHs a is negative and b is positive. This means that for HCSCs we have $\mu(\varepsilon_i) > \varepsilon_i$ while for EEHs we have either $\mu(\varepsilon_i) > \varepsilon_i$ or $\mu(\varepsilon_i) < \varepsilon_i$ depending on the values of a and b.

In EEHs the production of electrical work stems from the interaction of the CRM with an external field of photons. This interaction induces transitions of electrons that are in the high-energy levels (HELs) to low-energy levels (LELs). In both CC-EEHs and TRCs this interaction does the cell to radiate energy to the surroundings and cools down the electronic population that is in the emitter. In some cases, the cell reabsorbs some of the emitted photons what causes secondary excitations (see panel (c) of Fig. 1) and new photon emissions. Thus, the photon field near the EEH and the electron-hole population in the emitter are in equilibrium [42]. The equilibrium is expressed through the equation,

$$e_{i,HEL} \leftrightarrows e_{j,LEL} + h\nu. \quad (9)$$

Equation (9) shows that the cell-radiation interaction is well described as the interaction of a photon field with the electron-hole population of the cell. As in EEHs the temperature of the external field of photons is lower than the one of the electron-hole population, the equilibrium is described in terms of the chemical potentials as

$$\mu_\nu = \mu_e - \mu_h \quad (10)$$

Equation (10) shows that the chemical potential μ_ν of the photons emitted from the cell is equal to the difference between μ_e, the chemical potential of the electrons in the CB, and μ_h, the chemical potential of the holes in the VB.

In CC-EEHs the heat enters in the emitter with the electrons that get into it via a high energy selective contact as we show in Fig. 2. Thus, each electron that enters into the emitter has the energy ε_n that is bigger than μ_e, the average energy of the electronic population in the emitter. Since $\varepsilon_n \gg \mu_e$, the electrons entering into the emitter reduce their energy when they thermalize to the temperature of the other electrons that are in the emitter. In principle the electrons lose their energy in two ways: interacting with the lattice, i.e. via the electron-phonon coupling, or via radiative recombinations. The second mechanism causes the emission of photons from the EEHs [12]. As in EEHs the output power is proportional to the number of photons that are emitted from the cell [12] it is necessary to minimize the electron(hole)-phonon interaction, i.e. we need to avoid internal losses of energy. However, the electron-phonon can never be zero in EEHs so we must introduce the electron-phonon interaction in our equations. This is done assuming

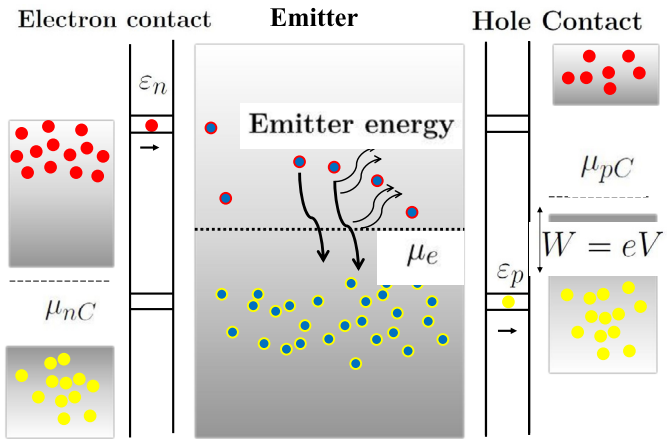

Fig. 2. Schematic representation of a CC-EEH with a metallic emitter. In the representation we include the electron and hole energy selective contacts, the chemical potentials of electrons and holes in the emitter and contacts and the cell output energy eV, where e is the electron charge. We also show that as $\mu_{pC} > \mu_{nC}$ the cell output energy is $eV < 0$. We also indicate how electrons de-excite from HELs to LELs when they are cooled down in the cell emitter. We also indicate that the energy that is lost by the electrons when they de-excitate from HELs to LELs is radiated to the cell surroundings.

that the phonons have a non-zero chemical potential μ_{phonon} what permits to write,

$$e_i + \text{phonon} \leftrightarrow e_j. \quad (11)$$

Equation (11) is rewritten in terms of the chemical potentials as,

$$a\varepsilon_i + b + \mu_{\text{phonon}} = a\varepsilon_j + b. \quad (12)$$

Equation (12) is satisfied for different energies ε_i and ε_j, a and μ_{phonon} so we can only have $a = 0$ and $\mu_{phonon} = 0$ as it happens in HCSCs [41]. Replacing $a = 0$ and $\mu_{phonon} = 0$ in (7) we obtain $T' = T$ what shows that if the electron-phonon interaction is strong then the temperature of the electrons in the emitter and in the contacts is the same. Having $T' = T$ reduces both the number of electrons that are emitted from the cell and the cell power [12]. Our discussion shows that to have EEHs able to produce big output powers we must minimize the electron-phonon interaction in them and advances that in TRCs, where the electron-phonon interaction is big, the temperature of the emitter is lower than in CC-EEHs. This implies that the output power of TRCs is necessarily smaller than that of CC-EEHs. We highlight that all these results are in agreement with Strandberg's [12] [13].

3. Cold-carrier energy-emissive harvesters

Let us now apply the CRM formalism to metallic and semiconductor CC-EEHs.

3.1. CC-EEHs with a metallic emitter

CC-EEHs with a metallic emitter have two parts: (i) a metallic emitter that optically couples the electronic population of the emitter with the field of photons surrounding the cell. (ii) Energy Selective Contacts (ESCs) that only allow the circulation of electrons having a fixed energy between the emitter and the contacts as we show in Fig. 2. Thus, the ESCs are used to inject hot electrons with the big thermal energy $\varepsilon_n \gg \mu_e$ from the left contact to the emitter and to withdraw from it cold ones with the lower energy $\varepsilon_p \ll \mu_e$. In this way the ESCs induce different chemical potentials μ_{nC} and μ_{pC} for electrons and holes in the contacts as we show in Fig. 2.

When the width (in energy) of the ESCs is much smaller than the thermal energy of the electrons in either the contacts and the emitter the following equation is satisfied [45]

Table 1. Maximum power, voltage for the maximum power and electronic temperature of metallic CC-EEHs. In the last column we present the electronic temperature of the converters in K.

E_c (eV.)	P_{max} (W/m^2)	V(P_{max}) (V)	V(P_{max}) (K)
0.05	12.54	−0.011	409.8
0.10	25.08	−0.022	409.8
0.15	37.63	−0.033	409.8
0.20	50.17	−0.044	409.8

$$\frac{\varepsilon_n - \mu_{nH}}{KT_H} = \frac{\varepsilon_n - \mu_e}{KT_C}, \tag{13}$$

for the energy ε_n at which electrons are injected into the emitter. Moreover, if we also admit that the width of the ESC of energy ε_p is small, then we are sure that

$$\frac{\mu_{pH} - \varepsilon_p}{KT_H} = \frac{\mu_e - \varepsilon_p}{KT_C} \tag{14}$$

is also satisfied.

Using (13) and (14) we obtain the cell output power $eV = \mu_{nH} - \mu_{pH}$

$$eV = (\varepsilon_n - \varepsilon_p)\left[1 - \frac{T_H}{T_C}\right]. \tag{15}$$

This equation shows that metallic CC-EEHs work as thermal emitters. Thus, their output work is the product of $\left[1 - \frac{T_H}{T_C}\right]$, a factor that depends on the temperatures T_H and T_C and $\varepsilon_n - \varepsilon_p$, the energy that is lost by each electron passing through the emitter. According to Strandberg equation (15) results when only the energy conservation principle (and not the detailed balance) is used to obtain the cell output power. However, we have shown that this equation is more fundamental as it is a consequence of having only one electronic population in the emitter and of using ESCs.

Some results that are obtained using this formalism can be found in Buddhiraju's [34] work. Thus, we know that metallic CC-EEHs working on Earth's surface that emit photons to the outerns space produce a maximum power of 48.4 W/m^2.

Some new results for metallic CC-EEHs are presented here. In the panel (A) of Fig. 3 we present the power-to-efficiency curves of several metallic CC-EEHs that have different contact energies E_c to show the effect of this parameter in both the power and the efficiency. In the panel (B) of Fig. 3 we see that cells working at $T_c = 600$ K working on the surface of the Earth produce powers that are around 70 W/m^2. We note that temperatures around 600 K are found in many industrial processes what shows the ability of metallic CC-EEHs to harness energy from the heat that is lost in industrial processes. Finally, Table 1 presents a summary of the possibilities of metallic CC-EEHs working at 500 K in ambients at 300 K. These results allow to understand the possibilities of metallic CC-EEHs to produce electrical power in ambients similar to those found in geothermal plants, that according to the data in the table produce powers of a few tens of W/m^2.

3.2. CC-EEHs with a semiconductor emitter

Let us now consider CC-EEHs that have a semiconductor emitter. In Fig. 4 we sketch their energy band structure and we show all the parameters that define their functioning. First we show that in semiconductor CC-EEHs the cell emitter has two different electron populations, one is in the VB and the other one is in the CB. The two populations are related because they exchange electrons but, as they are different, they are described using distinct Fermi-Dirac distributions. This model of EEHs is very suitable to describe cells where Auger recombinations and impact ionizations are important [42] but happen in a time-scale that is much slower than the one corresponding to the radiative recombinations. This means that each one of the two electron populations that exist in the emitter is in equilibrium on its own. Thus, electrons that are in energy levels $\varepsilon_i < E_G$ of the VB have the chemical potential μ_{iV} and electrons

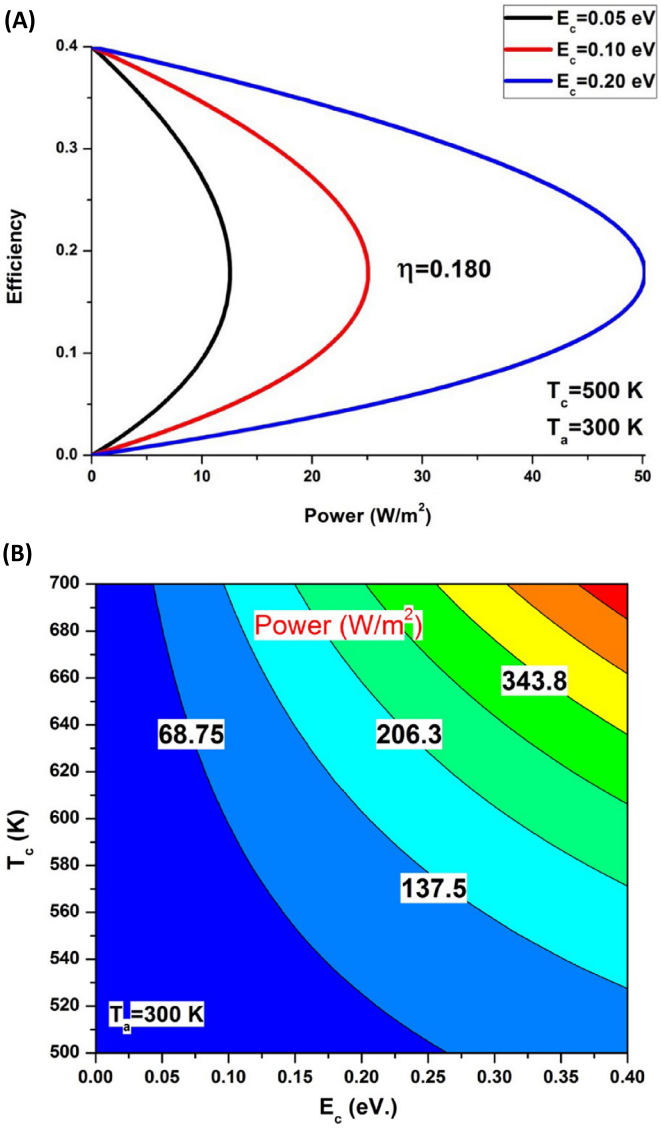

Fig. 3. Results for metallic CC-EEHs. In the panel (A) we present three power-efficiency curves for cells with $E_c = 0.05$, 0.10 and 0.20 eV. The three cells work at $T_C = 500$ K in an environment at 300 K. In the panel (B) we present a contour plot of the maximum power (in W/m^2) of CC-EEHs with contact energies between 0.0001 and 0.40 eV that work with $T_C \in (500, 700)$ K in an environment at 300 K.

that are in energy levels $\varepsilon_j > E_G$ of the CB have the different chemical potential μ_{jC}. μ_{iV} and μ_{jC} are different and they are related to ε_i and ε_j by the equations

$$\mu_{iV} = a_V \varepsilon_i + b_V \tag{16}$$

and

$$\mu_{jC} = a_C \varepsilon_j + b_C. \tag{17}$$

Here a_V and a_C are two constants that relate the chemical potentials $\mu_{(i,j)}$ and the energies $\varepsilon_{(i,j)}$. a_V defines the temperature of the electrons in the VB,

$$T_{e,VB} = \frac{T_c}{1 - a_V} \tag{18}$$

and a_C defines the temperature of the electrons in the CB,

$$T_{e,CB} = \frac{T_c}{1 - a_C}. \tag{19}$$

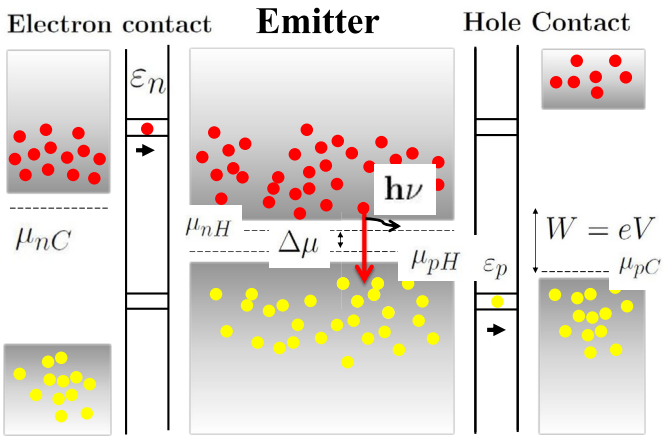

Fig. 4. Schematic representation of a CC-EEH with a semiconductor emitter. We include the electron and hole energy selective contacts (ESCs), the chemical potentials of electrons and holes in the emitter and contacts and the cell output power eV, where e is the electron charge. We show that as $\mu_{pC} > \mu_{nC}$ the cell output power is $eV < 0$. We also present how the de-excitation of electrons from the CB to the VB involves the emission of photons. Thus, the existence of a bandgap involves that there is a correspondence between the numer of emitted photons and the electronic current circulating through the cell emitter.

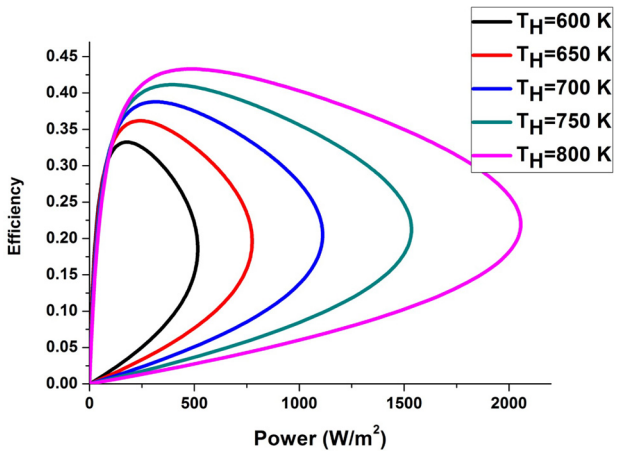

Fig. 5. Power-to-efficiency curves of some semiconductor CC-EEHs with $E_G = 0.1$ eV. In the figure P is in W/m^2. For all the calculations $T_C = 300$ K. In the table we present the maximum power (in W/m^2), the efficiency η_P at which the maximum power is delivered, the power that is produced at the maximum efficiency $P(max\ \eta)$ (in W/m^2) and the maximum efficiency Max.η.

Table 2. Maximum power (in W/m^2), the voltage (in V) at which that maximum power is delivered and the temperature T_e (in K) corresponding to that voltage of four CC-EEHs that work at 500 K in an ambient at 300 K.

$E_G = 0.1$	Max.P (W/m^2)	η_P	P(maxη) (W/m^2)	Max.η
$T_H = 600$ K	516.3	0.186	177.3	0.332
$T_H = 650$ K	775.4	0.195	245.2	0.362
$T_H = 700$ K	1111.3	0.203	317.7	0.388
$T_H = 750$ K	1534.2	0.213	398.7	0.414
$T_H = 800$ K	2055.0	0.220	487.9	0.433

Equations (18) and (19) show that the electrons that are in the VB and CB of semiconductor CC-EEHs can have different temperatures besides having different chemical potentials. However, as in CC-EEHs the two electronic populations are connected (mostly by radiative excitations and de-excitations) they are in equilibrium with the field of photons interacting with the emitter. This implies that the two effective temperatures must have to be equal, i.e. $T_{e,CB} = T_{e,VB}$, what makes $a_C = a_V$. However, as said, the two electronic populations are different what implies that $\mu_{iC} \neq \mu_{jV}$ because $b_C \neq b_V$. This is the important result: as in semiconductor CC-EEHs the electron populations in the VB and CB are different, the two populations have different chemical potentials and a split in the quasi-Fermi levels of value

$$\Delta\mu_v = \mu_{e,CB} - \mu_{e,VB} \tag{20}$$

exist in it. In other words, the photons that are emitted from semiconductor CC-EEHs have non-zero chemical potential. This model of CC-EHHs is known as the *particle conservation model for EEHs* [12] in reference to the equivalent model developed by Würfel [42] for HCSCs. In the work of Strandberg (20) is presented as a consequence of the use of the particle conservation principle to obtain the working properties of the cells. Here we have shown that its origin is found in having two electronic populations in the emitter that are connected by radiative transitions and that, at the same time, are in equilibrium with an external field of photons. Therefore, we think that the origin of equation (20) is more fundamental that the one that was given to it in Strandberg's work. Our formalism also clarifies that $\Delta\mu_v$ is not equal to the cell output energy qV as it is necessary to include in the energy balance of the cell the energy that is used to reversibly heat up the electrons in the ESC of energy ε_n and the energy that is involved in the reversible cooling of the electrons in the ESC of energy ε_p. This implies that to rightly obtain the current-voltage curves of CC-EEHs with $E_G \neq 0$ it is now required the use of (i) the energy conservation rule and (ii) a particle conservation law. Due to this we have now an extra degree of freedom to determine the value of $\Delta\mu_v$, the cell current and the output voltage.

The formalism presented here for semiconductor CC-EEHs has several drawbacks. As it happens in HCSCs, the new formalism can, in some situations, lead to inconsistencies when the value of the electronic temperature is calculated. If this happens, it is possible to obtain values of this temperature under the temperature of the field of photons that surrounds the cell. As far as we know, this effect has not been reported in the literature yet but we are quite sure that it will. In any case, we think that the precautions that should be taken in the use of the *particle conservation model* on semiconductor CC-EEHS are few as the method will only probably just fail in cells where the intraband scattering processes are at least as fast as the interband ones. That is, there will only be problems in semiconductor CC-EEHs where radiative processes are extremely slow. Finally, we note that using the particle conservation method allows to obtain higher efficiencies than the ones that are obtained when this method is not used. This result is not new, as it was found in previous works [13]. Here we give a physical explanation to it within the CRM model in order to show the possibilities of our formalism.

On the other hand, when the electron-phonon interaction becomes strong in the cell emitter, the coefficients a_V and a_C of the equations (18) and (19) are zero. This implies that $T_{e,VB} = T_{e,CB} = T_c$, i.e. when the electron-phonon coupling exists in the emitter its temperature decreases and becomes similar to that of the cell contacts. This reduces a lot the energy that electrons can lose in the emitter by emission explaining why semiconductor CC-EEHs perform worse that the metallic ones. Moreover, this is the cause why semiconductor CC-EEHS have smaller ouput powers and efficiencies than metallic CC-EEHs. Once more, we are theoretically explaining, within the CRM model, results that have been numerically found in previous works [12] but for which no physical explanations were addressed.

In Fig. 5 we present some efficiency-to-power curves of semiconductor CC-EEHs. For the representation we have chosen $E_G = 0.1$ and $T_C = 300$ K. We have used values of $T_H \in (600, 800)$ K. The graph shows the increase that happens in both the maximum power and efficiency when the temperature of the cell is increased. In the Table 2 we present the values of the efficiency at which the maximum power is produced and of the meximum efficiency to show that when T_H increases from 600 to 800 K η^P only increases from 0.186 to 0.220 but that the max-

imum efficiency of the cell increases much more as it changes from 0.332 to 0.433.

4. Thermoradiative cells

Let us now consider TRCs, i.e. EEHs based on semiconductor pn-junctions. TRCs are the counterparts of photovoltaic cells and are made with small bandgap semiconductors of $E_G < 0.3$ eV. In them one of the metallic contacts is connected to the CB of the n-side of the pn-juntion and the other one is connected to the VB of the p-side. In TRCs hot electrons are injected into the emitter CB, thermalize to the temperature of the emitter, de-excite radiatively to the VB and are heated up in this band to reach the outgoing metallic contact (see panel (a) of Fig. 1).

In TRCs the bandgaps are small so some of the electrons that are injected in HELs eventually go through intraband de-excitation processes resulting in the (undesired) excitation of electrons from the VB to the CB. In these circumstances, see the panel (c) of Fig. 1, the net current of electrons in the TRC reduces.

Moreover, as TRCs do not have ESCs the electrons pass almost freely from the cell contacts to the emitter and vice-versa. So, in TRCs the electrons in the VB, CB and in the contacts have the same Fermi-Dirac distributions. This implies that $a_V = a_C = 0$ and $T_{i,V} = T_{i,C} = T_H$. Note the difference with both the metallic and semiconductor CC-EEHs where we had $T_{i,V} = T_{i,C}$ but $T_{i,V} \neq T_H$ and $T_{i,C} \neq T_H$. Another consequence of allowing the electron transport between the emitter and the contacts in a wide range of energies is that now the electron-phonon interaction is strong. This is consistent with the condition $a_V = a_C = 0$ and does μ_{iV} to be independent of ε_i and μ_{jC} to be independent of ε_j. Therefore, in TRCS both μ_{iV} and μ_{jC} are constant and have the values,

$$\mu_{iV} = b_{VB} \qquad \text{and} \qquad \mu_{iC} = b_{CB}. \tag{21}$$

We note that in general $\mu_{iV} \neq \mu_{iC}$ because $b_{VB} \neq b_{CB}$.

Another important consequence of the existence of intraband processes is that there is no more a one-to-one correspondence between the number of recombinations and the number of photons that are emitted from the cell. Due to this, the equation resulting from the use of the detailed balance method is generalized to

$$e^{(1)}_{CB} \leftrightarrow \sum_I^M e^{(I)}_{VB} + \sum_I h\nu_I + e^{(2)}_{CB}. \tag{22}$$

This equation includes the possibility of having up to M (with $M > 1$) excitations caused by the injection of one electron in a HEL. It also shows that when this happens some electrons are excited from the VB to the CB reducing the cell current. This situation has not been studied before in works on TRCs as the effect of multiple excitations in TRCs is expected to be small. To check the importance of this effect in the performance of the TRCs we have calculated P and η for TRCs of bandgap $E_G = 0.10$ eV working with $T_H = 500$ K in an environment at $T_C = 300$ K. To better understand the impact of the multiple electron recombination processes we first carried out one calculation considering that the DBM applies assuming a one-to-one correspondence between the number of excitations/recombinations and that of absorbed/emitted photons. This calculation resulted in a maximum power $P_{max} = 185.83$ W/m^2 that is delivered at the efficiency $\eta^P = 0.1555$. When the calculation was repeated assuming that all the electrons that are injected with an energy $\varepsilon > 2E_G$ necessarily go through intra-band de-excitation processes (causing the excitation of electrons from the VB to the CB) we obtained a maximum power $P_{max} = 185.73$ W/m ^{2} and we found that it is delivered with the efficiency $\eta^P = 0.1514$. To be sure of these results we performed another calculation keeping equal all the parameters and raising the TRC temperature to $T_H = 1000$ K. The calculation of the maximum power and efficiency without considering intraband processes gave $P = 5751.55$ W/m^2 and $\eta^P = 0.2234$. When calculation was repeated considering the intraband processes it gave $P = 5751.04$ W/m^2 and $\eta^P = 0.2184$. As it is seen all our results confirm that multiple electronic excitations due to the injection of electrons in HELs have a very small negative impact on the working properties of TRCs.

5. Intermediate band thermoradiative cells

Here we consider IB-TRCs. IB-TRCs are based on the ideas used to study IB-photovoltaic cells [34, 40, 41, 42, 43, 44, 45, 46, 47, 48, 49, 50, 51, 52, 53]. In 2018 Ye at al [57] considered the working properties of IB-TRCs working under solar illumination. In [57] a set up of IB-TRCs that assumes that the IB material is sandwiched between two usual semiconductor materials is used. Thus, the emitter of the cell is formed by a material that has two energy bandgaps E_{G1} and E_{G2} as shown in the panel (d) of the Fig. 1 instead of having one. In IB-TRCs, as it happens in IB photovoltaic cells, the energy levels are grouped in the VB, IB and CB and electrons only pass from one band to another by radiative transitions. In this work we carry out the calculations using the same model used in Ye's work. We also note that this is also the setup that was used by Luque and Martí to study IB photovoltaic cells [40].

As we apply Luque's model for IB-TRCs we admit that the carriers populations of the three bands are in equilibrium [40]. This is equivalent to assume that the interband processes in the cell are fast enough to keep each band in its equilibrium state. We also suppose that the electronic transitions among the three bands are mostly radiative. This means that when they happen, energy is radiated from the cell. These requirements, that are presented here as necessary to have a good IB system are also of the main importance in TRCs. This leads to think that the combination of the IB and TRC concepts must work very well.

However, a close analysis of IB-TRCs reveals some problems. Several works on IB photovoltaic cells discuss that one of the requirements of IB-devices is that the electronic IB must have a dispersion in energy that is big enough to consider the group of states a band and not a set of impurity levels [40]. This is so because in cases where the dispersion of the band is small the new states appearing in the bandgap behave as impurity deep levels. In such cases a strong Shockley-Read-Hall (SRH) recombination is induced what is detrimental for the performance of the cells [54, 55, 56]. In TRCs, where the bandgap must be narrow ($\leqslant 0.30$ eV), it is almost impossible to have a wide IB. It is, therefore, to be expected that in IB-TRCs the rate of SRH recombinations is high. In TRCs with a wider bandgap (≥ 0.30 eV.) the IB is a more realistic possibility to improve the cell performance. However, as noted in Strandberg's work [13], TRCs with bandgaps bigger than 0.30 eV produce very small output powers. The introduction of the IB in those TRCs would indeed get better their performance but still in that situation the output power of the cells is expected to be very small. As a conclusion we say that it is not foreseen that TRCs having an IB work better than TRCs without IB.

The solution to the problems of the energy dispersion of the IB was presented in some works of Luque and Martí [54] where it is considered the use of IBs formed by quantum dot structures to reduce their energy dispersion of the IB. Although for TRCs this solution seems to be a very good one, a closer analysis reveals that this is not because TRCs are systems that work under very weak illuminations and in those conditions the effect of the IB on the cell power is very small [54]. So, we conclude that the presence of an IB in the cell emitter of TRCs not necessarily improves the output power.

To check if our reasoning on the effect of the IB on the output power of TRCs is right we present in Fig. 6 the output power of two TRCs and two IB-TRCs. In our calculations we used bandgaps between $E_G = 0.10$ and 0.30 eV, and the temperatures $T_C = 100$ (or 200) K, and $T_H = 500$ (or 1000) K. In the simulations of the IB-TRCs the position and width of the IB was optimized to have the maximum value of the output power. In all the cases the presence of the IB reduced the maximum output power. We also note that the powers that were obtained with the IB were a 40% lower than those obtained in systems without an IB. We

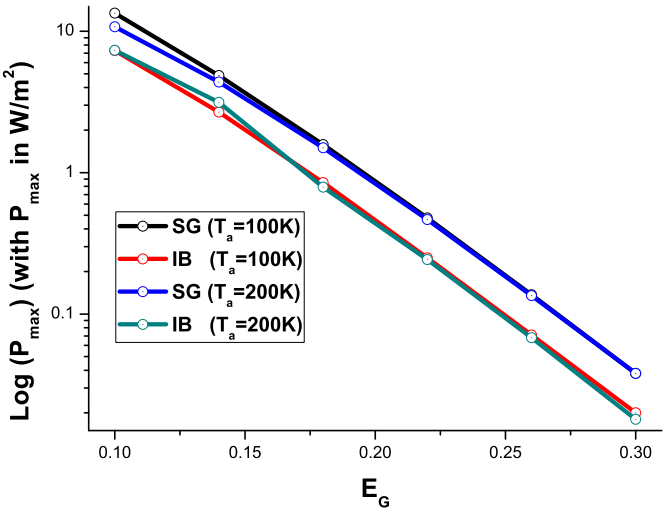

Fig. 6. Power (in W/m^2) of TRCs and IB-TRCs working in the surface of the Earth. We consider two temperatures $T_a = 100$ and 200 K for the environment and bandgaps between $E_G = 0.10$ and $E_G = 0.30$ eV. In the IB calculation the position and width of the IB is optimized.

also found, see the Fig. 6, that for a fixed value of E_G TRCs with and without the IB produce almost the same power.

Finally, we remark that in our model of IB-TRCs we did not include non-radiative processes due to two reasons. The first one is that we have followed the model of Luque et al. and in it non-radiative processes are ignored. The second one is that we did not include them as in section 4 we checked that their impact is very small in TRCs.

6. Summary

In summary we have adapted the formalism used by A. Luque and A. Martí to study solar converters to radiative ones. Moreover, we have shown that several types of radiative converters can be explained under a common model.

The model allows us to explain many of the previously published results based on the concept of energy emitter-harvesters. At the same time we were able to predict new results or to induce the limits of validity of some of the assumptions made in previous studies on EEHs. Thus, we showed that, (i) CC-EEHs with a metallic emitter work as thermal engines. (ii) CC-EEHs with a semiconductor emitter work as thermochemical engines. (iii) The particle conservation principle must be applied in semiconductor CC-EEHs as we have two electronic populations. (iv) The calculations carried out using the particle conservation principle should fail less in semiconductor CC-EEHs than in HCSCs. (v) We also checked that in semiconductor CC-EEHs the output voltage is different to the energy split between the Fermi levels of electrons in the VB and CB.

For TRCs we found that having a strong electron-phonon coupling is the reason why (i) the contacts and the emitter have the same effective temperature. We have also discussed how that coupling is also the reason why TRCs have much smaller efficiencies than CC-EEHs. Along this work, we also showed that in TRCs where multiple excitations exist the power is smaller than in TRCs where these processes do not exist.

Finally, we studied IB-TRCs. We showed that (i) although this concept is very attractive from a theoretical point of view, it is a very unrealistic concept from a technological one. (ii) In weak illumination conditions IB-TRCs work just as well as simple bandgap cells, or worse. This result, that contradicts those found in Ye's [57] work, is obtained in the specific conditions of TRCs that work on Earth's surface. We note here that we have chosen that working situation to show the ability of TRCs to produce electricity for regular use.

Declarations

Author contribution statement

J.J. Fernandez: Conceived and designed the experiments; Performed the experiments; Analyzed and interpreted the data; Contributed reagents, materials, analysis tools or data; Wrote the paper.

Funding statement

This work was supported by Ministerio de Ciencia, Innovación y Universidades (PID-2019-105182GB-I00).

Data availability statement

Data included in article/supplementary material/referenced in article.

Declaration of interests statement

The authors declare no conflict of interest.

Additional information

No additional information is available for this paper.

Acknowledgements

The author thanks Prof. J. E. Alvarellos and Drs. David García Aldea and E. M. Fernández and J. Rodríguez-Laguna for their help in the development of the work.

References

[1] S.J. Byrnes, R. Blanchard, F. Capasso, Harvesting renewable energy from Earth's mid-infrared emissions, Proc. Natl. Acad. Sci. 11 (2014) 3927.
[2] P. Berdhal, M. Martin, F. Sakkal, Thermal performance of radiative cooling panels, Int. J. Heat Mass Transf. 26 (1983) 871.
[3] A.R. Gentle, G.B. Smith, Radiative heat pumping from the using surface phonon resonant nanoparticles, Nano Lett. 10 (2010) 373.
[4] E. Rephaeli, A. Raman, S. Fan, Ultrabroadband photonic structures to achieve high-performance daytime radiative cooling, Nano Lett. 13 (2013) 457.
[5] A. Raman, M. Anoma, L. Zhu, E. Rephaeli, S. Fan, Passive radiative cooling below ambient air temperature under direct sunlight, Nature 515 (2014) 540.
[6] N. Nan, x.-C. Tsai, F. Camino, G.D. Bernanrd, N. Yu, R. Wehner, Keeping cool: enhanced optical reflection and radiative heat dissipation in Saharan silver ants, Science 349 (2015) 298.
[7] A.R. Gentle, G.B. Smith, A subambient open roof surface under the mid-summer sun, Adv. Sci. 2 (2015) 1500119.
[8] M.M. Hossain, B. Jia, M. Gu, A metamaterial emitter for highly efficient radiative cooling, Adv. Opt. Mat. 3 (2015) 1047.
[9] Y. Zhai, Y. Ma, S.N. David, D. Zhao, R. Lou, G. Tan, R. Tang, X. Yin, Scalable-manufactured randomized glass-polymer hybrid metamaterial for daytime radiative cooling, Science 355 (2017) 1062.
[10] K. Jl, Z. Jurado, Z. Chen, S. Fan, A.J. Minnich, Daytime radiative cooling using nearblack infrared emitters, ACS Photonics 4 (2017) 626.
[11] E.A. Goldstein, A.P. Raman, S. Fan, Sub-ambient non-evaporative fluid cooling with the sky, Nat. Energy 2 (2017) 17143.
[12] R. Strandberg, Heat to electricity conversion by cold carrier emissive energy harvesters, J. Appl. Phys. 118 (2015) 215102.
[13] R. Strandberg, Theoretical efficiency limits for thermoradiative energy conversion, J. Appl. Phys. 117 (2015) 055105.
[14] S.V. Boriskina, J.K. Tong, W.-C. Hsu, B. Liao, Y. Huang, V. Chiloyan, G. Chen, Heat meets light on the nanoscale, Nanophotonics 5 (1) (2016) 134–160.
[15] P. Santhanam, S. Fan, Thermal-to-electrical energy conversion by diodes under negative illumination, Phys. Rev. B 93 (2016) 161410.
[16] M.M. Hossain, M. Gu, Radiative cooling: principles, progress, and potentials, Adv. Sci. 3 (2016) 1500360.
[17] C. Lin, B. Wang, K.H. Teo, Z. Zhang, Performance comparison between photovoltaic and thermoradiative devices, J. Appl. Phys. 122 (24) (2017) 243103.
[18] T.J. Liao, X. Zhang, X.H. Chen, B.H. Lin, J.C. Chen, Negative illumination thermoradiative solar cell, Opt. Lett. 42 (16) (2017) 3236.

[19] X. Zhang, W. Peng, J. Lin, X. Chen, J. Chen, Parametric design criteria of an updated thermoradiative cell operating at optimal states, J. Appl. Phys. 122 (2017) 174505.
[20] J.J. Fernandez, Endoreversible model of thermal to radiative energy converters, J. Appl. Phys. 123 (2018) 164501.
[21] X. Sun, Y. Sun, Z. Zhou, M.A. Alam, P. Bermel, Radiative sky cooling: fundamental physics, materials, structures, and applications, Nanophotonics 6 (2017) 997.
[22] A.P. Raman, W. Li, S. Fan, ThermoRadiative cell – A new waste heat recovery technology for space power applications, in: AIAA Propuls. Energy Forum Expo 2019, 2019, p. 3977.
[23] J. Wang, C.H. Chen, R. Bonner, W.G. Anderson, ThermoRadiative cell - A new waste heat recovery technology for space power applications, in: AIAA Propuls. Energy Forum Expo 2019, 2019, p. 3977.
[24] T. Liao, Z. Yang, X. Chen, J. Chen, Thermoradiative-photovoltaic cells, IEEE Trans. Electron Devices 66 (3) (2019) 1386.
[25] E.J. Tervo, W.A. Callahan, E.S. Toberer, M.A. Steiner, A.J. Ferguson, Solar thermoradiative-photovoltaic energy conversion, Cell Rep. Phys. Sci. 1 (2020) 100258.
[26] W. Li, S. Buddhiraju, S. Fan, Thermodynamic limits for simultaneous energy harvesting from the hot sun and cold outer space, Light Sci. Appl. 9 (1) (2020) 1.
[27] N.J. Ekins-Daukes, M.H. Sazzad, L.Al. Kiyumi, M. Nielsen, P. Reece, A. Mellor, M.A. Green, A. Pusch, Generating power at night using a thermoradiative diode, how is this possible?, in: 47th IEEE Photovolt. Spec. Conf., 2020, p. 2214.
[28] T. Deppe, J.N. Munday, Nighttime photovoltaic cells: electrical power generation by optically coupling with deep space, ACS Photonics 7 (2020) 1.
[29] X. Yin, R. Yang, G. Tan, S. Fan, Terrestrial radiative cooling: using the cold universe as a renewable and sustainable energy source, Science 370 (2020) 786.
[30] M.P. Nielsen, A. Pusch, M.H. Sazzad, P.M. Pierce, P.J. Recce, N.J. Ekins-Daukes, Thermoradiative power conversion from HgCdTe photodiodes and their current-voltage characteristics.
[31] J.J. Fernández, Thermoradiative energy conversion with quasi-Fermi level variations, IEEE Trans. Electron Devices 64 (2017) 250.
[32] W.-C. Hsu, J.K. Tong, B. Liao, Y. Huang, S.V. Boriskina, G. Chen, Entropic and near-field improvements of thermoradiative cells, Sci. Rep. 6 (1) (2016) 34837.
[33] J.J. Fernández, Emissive-energy harvesting using near-field heat transfer, Eng. Res. Express 2 (2020) 015040.
[34] S. Buddhiraju, P. Santhanam, S. Fan, Thermodynamic limits of energy harvesting from outgoing thermal radiation, Proc. Natl. Acad. Sci. 115 (16) (2018) E3609.
[35] M. Ono, P. Santhanam, W. Li, B. Zao, S. Fan, Experimental demonstration of energy harvesting from the sky using the negative illumination effect of a semiconductor photodiode, Appl. Phys. Lett. 114 (2019) 161602.
[36] F. Chen, A.N. Cartwright, H. Lu, W.J. Schaff, Time-resolved spectroscopy of recombination and relaxation dynamics in InN, Appl. Phys. Lett. 83 (Dec 2003) 4984.
[37] G. Conibeer, S. Shrestha, S. Huang, R. Patterson, H. Xia, Y. Feng, P. Zhang, N. Gupta, M. Tayebjee, S. Smyth, Y. Liao, S. Lin, P. Wang, X. Dai, S. Chung, Hot carrier solar cell absorber prerequisites and candidate material systems, Sol. Energy Mater. Sol. Cells 135 (2014) 124.
[38] P.G. Klemens, Anharmonic decay of optical phonons, Phys. Rev. 148 (2) (1966) 845–848.
[39] B.K. Ridley, The LO phonon lifetime in GaN, J. Phys. Condens. Matter 8 (1996) L511–L513.
[40] A. Luque, A. Martí, Increasing the efficiency of solar cells by photon induced transitions at intermediate levels, Phys. Rev. Lett. 78 (1997) 5014.
[41] A. Martí, A. Luque, Electrochemical potential (quasi-Fermi levels) and the operation of hot-carrier, impact-ionization and intermediate-band solar cells, IEEE J. Photovolt. 3 (2013) 1298.
[42] P. Würfel, A.S. Brown, T.E. Humphrey, M.A. Green, Particle conservation in hot-carrier solar cells, Prog. Photovolt. Res. Appl. 13 (2005) 277–286.
[43] P. Würfel, Solar energy conversion with hot electrons from impact ionisation, Sol. Energy Mater. Sol. Cells 46 (1997) 43.
[44] G. Conibeer, J.F. Guillemoles, M.A. Green, Phononic bandgap engineering for hot-carrier solar cell absorbers, in: Proc. 20th Eur. Photovoltaic Solar Energy Conf. 35, 2005.
[45] A.N. Jordan, B. Sothmann, R. Sánchez, M. Büttiker, Powerful and efficient energy harvester with resonant-tunneling quantum dots, Phys. Rev. B 87 (2013) 075312.
[46] J.J. Fernández, Limiting output voltage of isentropic energy emissive harvesters, J. Appl. Phys. 128 (2020) 044501.
[47] A. Luque, A. Marti, A metallic intermediate band high efficiency solar cell, Prog. Photovolt. Res. Appl. 9 (2001) 73–86.
[48] A.M. Green, Multiple band and impurity photovoltaic solar cells: general theory and comparison to tandem cells, Prog. Photovolt. Res. Appl. 9 (2001) 137–144.
[49] N.J. Ekins-Daukes, C.B. Honsberg, M. Yamaguchi, Signature of intermediate band materials from luminescence measurements, in: Proc. 31st IEEE Photovoltaic Specialists Conf., 2005, p. 49.
[50] A. Marti, L. Cuadra, A. Luque, Quantum dot intermediate band solar cell, in: Proc. 28th IEEE Photovoltaics Specialists Conf., IEEE, 2001, p. 904.
[51] A. Luque, et al., General equivalent circuit for intermediate band devices: potentials, currents and electroluminescence, Appl. Phys. 96 (2004) 903.
[52] A. Marti, et al., Elements of the design and analysis band solar of quantum-dot intermediate cells, Thin Solid Films 516 (2008) 6716.
[53] R. Strandberg, T.M. Reenaas, Photofilling of intermediate bands, Appl. Phys. 105 (2009) 124512.
[54] A. Luque, A. Martí, The intermediate band solar cell: progress toward the realization of an attractive concept, Adv. Mater. 22 (2009) 160–174.
[55] A. Martí, L. Cuadra, A. Luque, Quantum-dot intermediate band solar cell, in: Conference Record of the Twenty-Eighth IEEE Photovoltaic Specialists Conference - 2000, 2000 (Cat. No. 00CH37036).
[56] A. Luque, P.G. Linares, E. Antolín, E. Cánovas, C.D. Farmer, C.R. Stanley, A. Martí, Multiple levels in intermediate band solar cells, Appl. Phys. Lett. 96 (2010) 013501.
[57] Z. Ye, W. Peng, S. Su, J. Chen, Intermediate band thermoradiative cells, IEEE Trans. Electron Devices 65 (2018) 5428.